Untethered Single Cell Grippers for Active Biopsy

Qianru Jin,[1, ∀] Yuqian Yang,[1] Julian A. Jackson,[1] ChangKyu Yoon,[2, #] David Gracias[1, 2, *]

[1]Department of Chemical and Biomolecular Engineering, Johns Hopkins University, Baltimore, Maryland 21218, USA
[2]Department of Materials Science and Engineering, Johns Hopkins University, Baltimore, Maryland 21218, USA

[∀]Present address: Disease Biophysics Group, John A. Paulson School of Engineering and Applied Sciences, Harvard University, Cambridge, MA 02138, USA
[#]Present address: Department of Mechanical Systems Engineering, Sookmyung Women's University, Seoul, 04310, Republic of Korea

TOC Figure

Abstract

Single cell manipulation is important in biosensing, biorobotics, and quantitative cell analysis. Although microbeads, droplets, and microrobots have been developed previously, it is still challenging to simultaneously excise, capture, and manipulate single cells in a biocompatible manner. Here, we describe untethered single cell grippers, that can be remotely guided and actuated on-demand to actively capture or excise individual or few cells. We describe a novel molding method to micropattern a thermally responsive wax layer for biocompatible motion actuation. The multi-fingered grippers derive their energy from the triggered release of residual differential stress in bilayer hinges composed of silicon oxides. A magnetic layer enables remote guidance through narrow conduits and fixed tissues sections *ex vivo*. Our results provide an important advance in high-throughput single cell scale biopsy tools important to lab-on-a-chip devices, microrobotics, and minimally invasive surgery.

Keywords: biomedical engineering, molding, robotics, drug delivery, tissue sampling, genomics, proteomics

Untethered miniaturized devices that can manipulate single cells with high accuracy and reproducibility, hold great promise in robotics, surgery and biomedical engineering.[1-3] Conventional surgical and biopsy devices rely on catheters and endoscopes to navigate through the gastrointestinal, urological, and cardiovascular passageways. However, these processes limit accessibility and often require entry point lesions, cause patient discomfort and collateral damage.[4] Many diseased tissues are highly heterogeneous at the single cell level.[5, 6] Untethered microrobotic devices that can operate at the single cell can open up access to narrow conduits, minimize invasiveness, and enhance the accuracy and efficacy of tissue sampling and surgical interventions.

In vitro biomedical applications such as microdissection, assisted reproductive technology, and somatic cell nuclear transfer could benefit tremendously from single cell manipulators, where high resolution controlled motion could improve efficiency and minimize manual variances.[7, 8] Present-day single cell analysis methods that utilize droplet microfluidics or microbeads to separate cells, are passive and require preparatory procedures for tissue isolation and labeling.[9] Laser-capture microdissection isolates tissues of interest by laser cutting in a microscopic field, albeit with low throughput and relatively compromised sample quality.[9] High-throughput active single cell devices could significantly enhance parallel isolation and analysis of microscale tissues. Furthermore, single cell manipulation could maneuver cells with 3D precision for building multicellular architectures.[10]

Substantial progress has been made in developing single cell sized manipulators, enabled by innovations in miniaturization and energy utilization. Untethered single cell devices provide advantages over wired devices especially in applications which require parallel operation off-chip. However, due to their untethered nature and small size, the energy required for actuation and motion needs to be delivered wirelessly which presents a formidable challenge. Chemically powered microrobots have achieved considerable success *in vitro* and *in vivo*, but they often require highly specialized environment, non-biocompatible solvents and onboard chemical fuels.[11-13] Elsewhere, energy delivered through ultrasound[14] or electromagnetic fields,[15, 16] has been used for cell locomotion, biosensing, tissue cutting, and biomolecular delivery.[8, 16-20] However, their motions are largely limited to translation and rotation, such as

pulling or tumbling of isolated cells,[19] or drilling and cleaving of *ex vivo* tissues.[12, 20] This constrained motion limits their applicability to simple tasks and makes it challenging to realize dexterous motions in complex environments such as *in vivo* conduits. Hence, there is a need to develop microrobots that can provide multidimensional motion, movable subunits, swift navigation, and precisely controlled interaction with cells, in a biocompatible environment. Significant technical challenges need to be overcome to create untethered robots with biocompatible and potentially biodegradable materials, to provide energy and guidance from afar, to trigger on-demand actuation, and to integrate these functions at single cell scale.

Here, we address some of these challenges by developing untethered thermo-responsive single cell grippers that employ residual stress powered actuators[21-24] with the introduction of several important advances. First, we integrate a biocompatible thermally responsive layer to enable controlled on-demand actuation. After experimenting with a range of materials, we chose paraffin wax and developed a protocol to micropattern this phase-changing material. As compared to the previously utilized triggers made of photoresist,[24] the bioinert paraffin wax can minimize cytotoxicity. We rationally optimize the design to enable thermally triggered actuation at a cell-friendly biocompatible temperature. Second, we incorporate an iron layer to enable magnetic manipulation from afar. Previous single cell grippers were operated in on-chip arrays, where the gripping motion was controlled by tuning the dissolution rate of a sacrificial layer for passive cell trapping.[21-23] Our newly incorporated functional layers allow the grippers to remain open even upon release from the substrate, so they can be utilized for active on-demand cell capture off-chip. Finally, we demonstrate navigation through complex narrow conduits, targeted capture of single live cells, and biopsy at the micrometer (a few cells) scale. As compared to previously demonstrated grippers that were used to biopsy hundreds of cells,[24] the current gripper size has been scaled down significantly in all dimensions, with a tip-to-tip size of 70 μm when open and 15 μm after folding, and we have demonstrated single (or a few) cell excision with significantly enhanced spatial resolution.

We needed to incorporate a stimuli-responsive trigger to enable on-demand activation of the untethered grippers and chose paraffin wax as the functional material for a variety of reasons. First, wax is chemically and biologically inert and biocompatible[25] and widely used in food products (e.g. cheese) and

food processing (e.g. wax paper). Second, technical grade paraffin wax which is a mixture of alkanes with chemical formula of C_nH_{2n+2} ($20<n<40$) exhibits a range of phase-transition temperatures of relevance to biology and the human body.[26] Paraffin has been used previously in microfluidic pumps to provide large thrust, due to its significant solid-to-liquid volume expansion. Previously reported paraffin microfabrication involved the manual deposition of volumes of >1 mm^3 and were somewhat imprecise or complicated.[27] Elsewhere, paraffin micropatterning at lateral dimensions of 400-600 μm was achieved, but the process required several steps of microfabrication with customized specialized equipment.[28]

Here, we developed a novel molding approach to pattern paraffin wax at the microscale, adapted from prior and ongoing efforts in our laboratory.[29] Our approach is straightforward, compatible with conventional microfabrication process, and we can create paraffin micropatterns with lateral dimensions ranging from 1 mm to 10 μm (or potentially smaller depending on the mold size) and uniform thickness in the range of micro- and sub-micrometers. The process flow is illustrated in **Figure** 1a. Briefly, we first photopatterned and deposited a differentially stressed bilayer composed of silicon monoxide and silicon dioxide. The triggered release of the stored differential stress provides the energy for the gripping motion. Second, we photopatterned and deposited relatively thick segments of silicon dioxide to provide the structural rigidity with a thin iron layer for magnetic response. Finally, for paraffin patterning, we fabricated a mold of a negative photoresist pattern. We then melted the paraffin wax and spin coated it at 140ºC while it was a viscous liquid over the photoresist molded patterns. After the silicon wafer cooled down and the wax solidified, we dissolved the photoresist mold by a gentle wash in acetone and isopropanol. The residual solid paraffin wax took the shape of the negative mold patterns defined by the photoresist.

To visualize the paraffin wax layer which is transparent under visible light illumination, we imaged the grippers by scanning electron microscopy (SEM). **Figure** 1b shows SEM image of a gripper with the 30 nm thin stress layer (zoom-in in **Figure** 1c) and rigid panels prior to wax patterning. We patterned the wax layer, which appears dark in color in the SEM image in **Figure** 1d only on top of the grippers and it completely covers the hinges with a thickness of about 1 μm (**Figure** 1e). The optical image in **Figure** 1f shows an array of the grippers after fabrication. We observed that the hinges were transparent in optical

images due to the transparency of SiO, SiO_2, and wax; while the rigid arms were opaque due to the iron layer. We note that all steps of the fabrication process are compatible with conventional very large-scale integration (VLSI) and scalable, as seen from the large array of uniformly patterned paraffin on top of the grippers in **Figure** 1g. It is also noteworthy that our patterning method is versatile and could be applied to other phase changing biocompatible trigger materials. For example, we also successfully patterned food grade butter with a similar resolution (**Figure** S1).

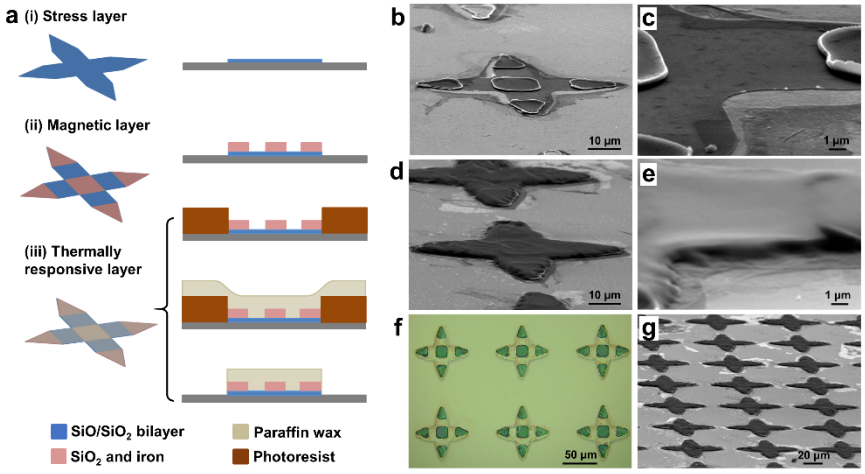

Figure 1. Fabrication of single cell grippers with magnetic response and a thermally responsive trigger. **(a)** Schematics of the fabrication process for single cell grippers which include the following steps, (i) photolithography and deposition of the silicon monoxide (SiO) and silicon dioxide (SiO_2) bilayer as the stress layer; (ii) photolithography and deposition of silicon dioxide and iron as the rigid segments for magnetic response; (iii) patterning of the paraffin layer by photoresist molding, paraffin spin coating and lift-off. **(b-c)** SEM image of (b) a gripper without the paraffin layer, and (c) a zoom-in view at the hinge. **(d-e)** SEM image of (d) a gripper with paraffin layer, and (e) a zoom-in view at the hinge. **(f)** Optical image of an array of single cell grippers, with rigid iron segments and transparent (SiO/SiO_2) bilayer hinges; the transparent paraffin layer covers the entire gripper. **(g)** SEM image of a large array of grippers with a patterned paraffin layer on top.

To realize a functional gripping action at such a small size scale, we needed to carefully optimize the materials and design parameters. The magnitude of the change of Young's moduli of paraffin at different temperatures is critical for the thermal actuation of gripping motion. At low temperature, the rigid paraffin prevents the bilayer hinge from folding. As the temperature increases, the total bending rigidity of the hinge decreases due to the decreased Young' modulus of paraffin. Once the residual stress outweighs the decreasing bending rigidity, the gripper will close. We measured the stress-strain curve of paraffin at 26°C and 37°C by Dynamic Mechanical Analysis (DMA). **Figure** 2a shows Young's modulus decreased

significantly from 6.44 MPa at 26°C to 0.37 MPa at 37°C. These measured values are in qualitative agreement with the range in the literature and the differences can be attributed to differences in the wax composition at different temperatures.[30, 31]

The bending curvature of the multilayered structures depends on the stress, thickness, and mechanical properties of the materials in each layer.[32] The thickness of each layer can be tuned during the deposition steps to achieve the desired fold angles. To determine the optimal paraffin thickness, we adopted an analytical model to predict the fold angle with respect to varying paraffin thicknesses at 26°C and 37°C, using the measured wax modulus and the bilayer stress measured previously,[21] as shown in **Figure** 2b. For both temperatures, we observed that the fold angle decreases as the paraffin layer thickness increases, due to the increased bending rigidity. At the same paraffin thickness, we observed that the difference between the fold angles at the two temperatures was crucial to determine the working range of the gripper. We found that a paraffin thickness range between 0.5-1 μm was optimal as indicated by the shaded area, i.e. small fold angle at low temperature, and large fold angle at high temperature. A gripper with a thinner paraffin layer will close at the lower temperature, while a gripper with a thicker layer will not close at the higher temperature. Finite element modelling (FEM) in **Figure** 2c shows folding states of the grippers with two different paraffin thicknesses (0.6 μm and 0.9 μm) and an optimal range of fold angles below (26°C) and at the trigger (37°C) temperature. Based on the analysis, we chose this paraffin thickness range between 0.6 μm and 0.9 μm in our subsequent experiments.

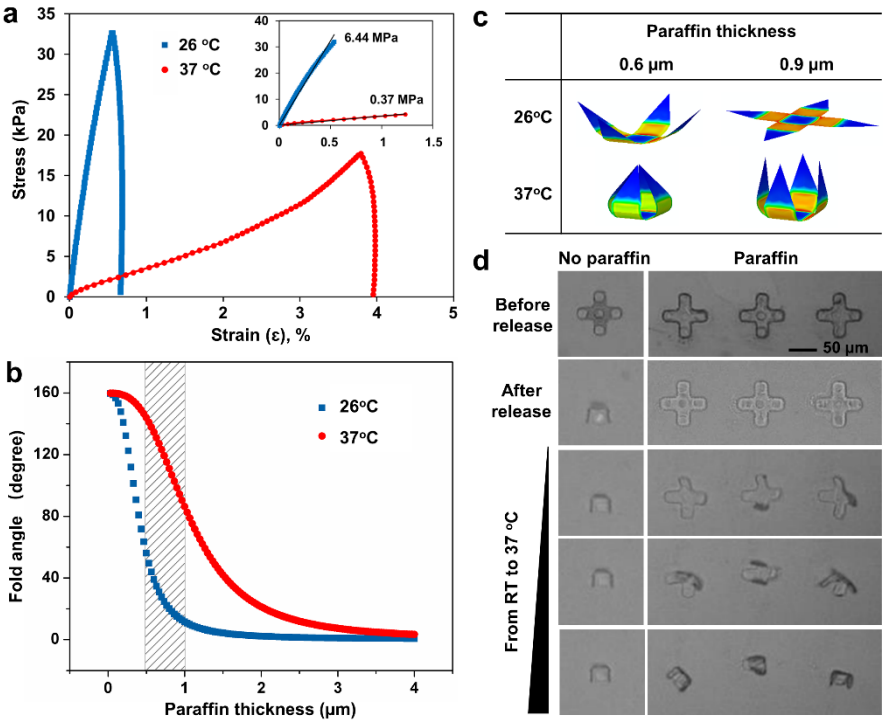

Figure 2. Mechanical characteristics of the paraffin wax trigger and fold angle optimization of the single cell grippers. (a) Stress/strain curve for paraffin wax at temperatures of 26°C and 37°C based on DMA measurement. Inset shows the initial linear range. **(b)** Analytical study of the fold angle of single cell grippers as a function of paraffin thickness at 26°C and 37°C, based on the analytical solution from reference.[32] **(c)** Finite element simulation snapshots of single cell grippers with two different wax thicknesses at 26°C and 37°C. **(d)** Folding process of single cell grippers before release, after release, and during the heating process from room temperature to 37°C. The gripper in the left column did not have paraffin layer; the three grippers in the right column had paraffin layer on top as indicated by the dark edge and coating all over the gripper in the first row.

We experimentally verified the self-folding process with and without the trigger. In **Figure** 2d, initially all grippers stayed open on the substrate before release. Once, we dissolved the sacrificial layer, all grippers got released from the substrate. Among them, the grippers without the paraffin layer closed instantaneously, but those coated with the paraffin layer remained open. As the temperature increased from 26°C to 37°C, the grippers with the paraffin layer gradually started to close. This study shows that a trigger layer is essential for on-demand thermally responsive actuation at a specific location and time. Moreover, by engineering an actuation temperature of 37°C we ensure that the process is thermally biocompatible. In screening materials for the trigger layer, we found that food-grade butter could also be patterned and used as a trigger layer for thermo-responsive actuation at 37°C (**Figure** S1).

Scaled down from the previously developed gastrointestinal tract biopsy grippers of 0.25-1 mm size,[24, 33] our single cell grippers feature a tip-to-tip open size of 70 μm, comparable to the size of human arterioles (50-300 μm).[34] To introduce the capability of remote controlled motion, we equipped the grippers with an iron layer for locomotion using a magnetic field. We deposited 100 nm iron at the rigid segments by e-beam evaporation, so the iron layer could provide sufficient magnetization without affecting folding at the hinge. We note that it is a major challenge to move microscale objects at low Reynolds number, due to significant amount of drag experienced by the object at these small scales. Based on the geometry, material properties and an estimated drag coefficient,[33, 35, 36] we calculated that the minimal magnetic field required to power the single cell gripper is on the order of milli T/m (see SI for more details), which is much smaller than the typical gradient field 0.1 T/m used in clinical magnetic resonance imaging (MRI) systems. This feature highlights the potential to use MR for *in vivo* locomotion of the single cell grippers in clinical settings. For simplicity, we used a laboratory bar magnet in our study and demonstrated that we could move the grippers with a velocity up to 100-150 μm/s in PBS buffer in microfluidic channels.

To highlight their small size and the ability to locomote in a complex conduit, we steered an untethered gripper in an *ex vivo* fixed human fallopian tube tissue section (**Figure** 3a). We could move the gripper to access different locations in the tissue section following a guided path. **Figure** 3b shows temperature triggered folding at the bifurcation site of the conduits. Upon reaching the bifurcation site (i), we increased the temperature to trigger the gradual close of the gripper (ii-iv). Afterwards, we steered the gripper away along the conduit (**Figure** 3c). In addition to guidance in biological conduits, we were able to move the grippers in complex microfluidic channels with widths <150 μm, including bifurcating, zigzag, winding and twisted channels, and channels with multiple exits (**Figure** S2). The ability to navigate through such complex channel geometries highlights accessibility in hard-to-reach spaces which is important for lab-on-a-chip, robotic and *in vivo* applications.

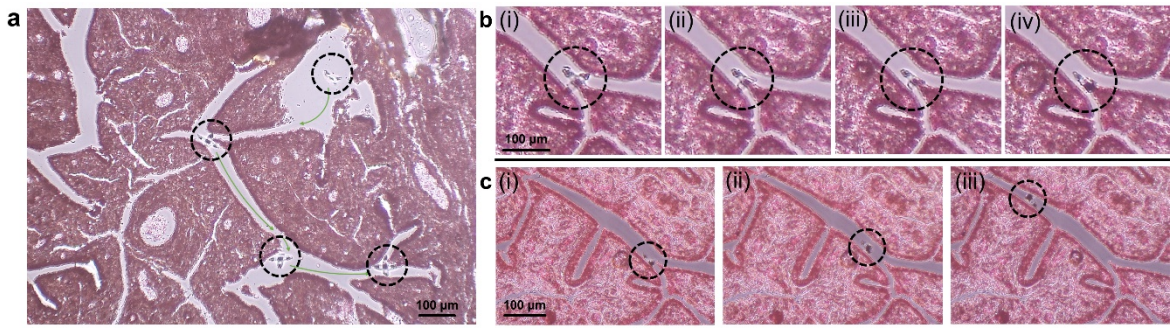

Figure 3. Guided navigation of a single cell gripper through fixed human fallopian tube tissue.
(a) An open gripper moving in a slice of *ex vivo* human fallopian tube tissue, guided by a gradient magnetic field. **(b)** (i-iv) Optical snapshots show the gripper actuation upon temperature increase at the bifurcation site within the biological conduits. **(c)** (i-iii) Optical snapshots show the closed gripper being navigated leaving the biological conduit. The hematoxylin and eosin (H&E) stained tissue slice was dissembled from a commercially available microscope slide.

We anticipate that these untethered, thermally responsive grippers can be used to manipulate biological cargo such as single cells with high precision and biocompatibility. We performed capture of a single MDA-MB-231 human breast cancer cell from a distance (**Movie** S1). We guided the gripper magnetically and gradually approached the cell periphery (**Figure** 4a). Upon final position adjustment in **Figure** 4b (i), we increased the temperature to trigger folding (ii-iii) until the target cell was captured (iv). We were able to capture and transport the cell to any desired position (**Figure** 4c). Since we designed the grippers so that we can actuate folding around 37°C, the cell capture process is biocompatible. We verified viability using a live/dead assay which shows that the target cell was alive during the actuation process, indicated by the green fluorescence from calcein AM staining (**Figure** 4d). More details are in the supporting methods and **Figure** S4. Apart from cells, we verified that the grippers were strong enough to capture and transport significantly stiffer cargo such as 15 µm polystyrene beads (**Figure** S3), which could be challenging for some soft microrobots. Since the grippers are fabricated using silicon oxides and paraffin, they are chemically inert and can withstand many harsh chemicals and organic solvents. Hence, the grippers are not only able to grip delicate biological cargo but can also be used with a range of alternate cargo in a wide range of chemical environments.

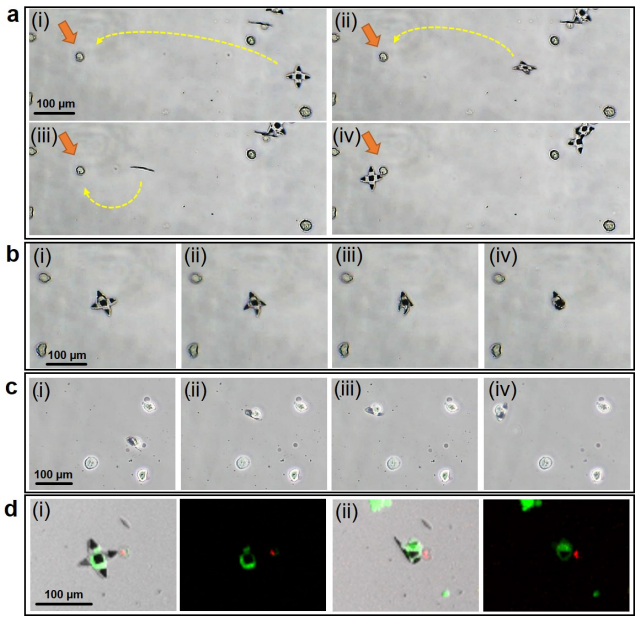

Figure 4. Approach and capture of a single cell using the thermo-responsive grippers. (a) (i-iv) Optical images show a 70 µm tip-to-tip sized gripper being guided by magnetic field and approaching a targeted cell from a distance. **(b)** (i-iv) On reaching the targeted cell, the gripper was actuated by increasing field temperature. **(c)** (i-iv) The gripper captured the single cell, and carried the cell away guided by magnetic field. **(d)** A Live/Dead assay was performed on the cells (i) before and (ii) after the actuation of grippers. The green fluorescence indicates that the cell was alive after capture. Green and red fluorescence resulted from staining by calcein AM (live, green) and ethidium homodimer (dead, red). Suspended MDA-MB-231 cells were used in this experiment.

Of relevance to surgery, and in contrast to other passive manipulators such as beads and microdroplets, our grippers have movable appendages which can be used to excise and grasp objects for completing tasks such as biopsies or cell excision from tissue samples. We first applied the grippers for cell excision from a cluster of fibroblasts resembling a laboratory tissue sample. As shown in **Figure** 5 and **Movie** S2, we deployed the gripper from a distance (i), moved the gripper to approach the cell cluster (ii), and positioned the gripper at the branch of the cluster (iii). At this point, we began to increase the field temperature when the gripper was positioned properly. The gripper started to close, and successfully captured a few cells at the side (iv). Next, we switched the magnetic field direction, to pull the captured cells away from the cluster (v). We observed that the captured cells were primarily connected to the bulk cluster by association with extracellular matrix. By steering the gripper with the captured cells in different directions, we created a strong twisting motion to separate the cells from the cluster and transport them

away (vi). This process highlights the dexterity of motion and the firm grasp of cells by the grippers, which is essential for surgical operations with high precision at single cell length scales. Also, grippers permit visualization of cellular components. **Figure** 5b shows fluorescence images of, (i) a single cell, and (ii) two cells captured from a cell supension within the folded gripper arms. The suspended cells were previously stained to resolve detailed cellular features including the nuclei (DAPI, blue) and cytoskeleton (microtubules, antibody labeling, green). **Figure** S5 shows gripping of food-grade chicken liver tissue *ex vivo*.

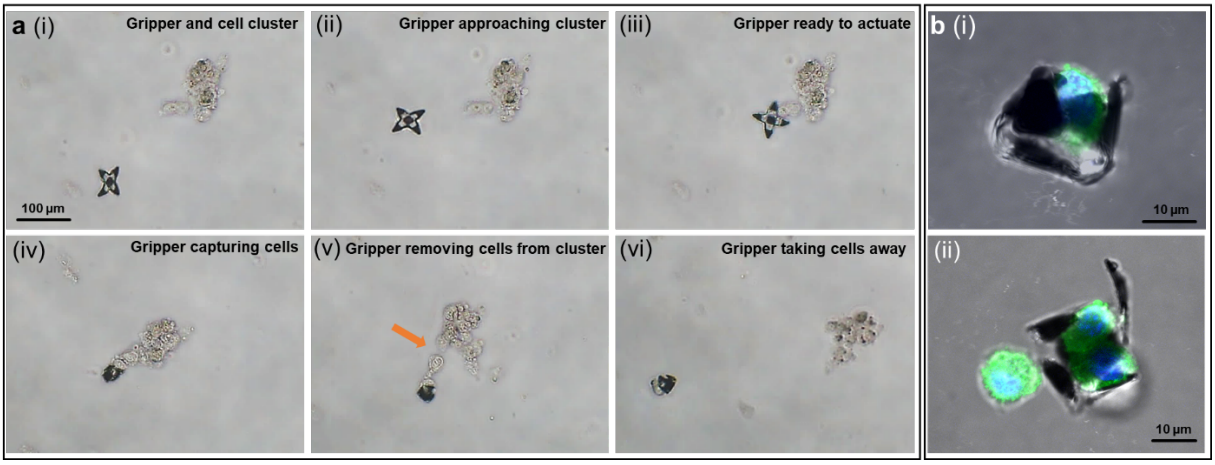

Figure 5. Few-cell biopsy from a cell cluster and visualization of cellular components of captured suspended cells. **(a)** The process of a gripper capturing and excising cells from a cell cluster in the following steps, (i) a gripper and a cell cluster at a distance; (ii) the gripper approached the cell cluster guided by magnetic field; (iii) the gripper reached the desired location; (iv) upon temperature increase, the gripper grasped a few cells; (v) the gripper was dragging the captured cells away from the cluster by changing directions of magnetic field; (vi) the gripper successfully excised cells and moved them away. **(b)** Immunofluorescence images of suspended fibroblast cells captured by the grippers: (i) side view of a captured single cell, (ii) two cells captured inside a gripper. Cells were fixed and stained for nuclei (DAPI, blue), and β-tubulin (antibody labeling, green).

In summary, we have described a new class of untethered, thermal responsive grippers, that can capture single live cells and perform excision of few cells from cell clumps. Our devices feature extremely small size, controlled actuation and locomotion, dexterous motion, biocompatibility, and high throughput fabrication, providing a new strategy of microscale robotic manipulation with enhanced sophistication.

The small single cell size, scalable fabrication process and possibility for further miniaturization[21] opens up new opportunities for *in vivo* access beyond the GI tract as demonstrated previously,[24] such as

human arterioles (50-300 μm), ureters (3-4 mm) and mammary lactiferous ducts (1-2 mm). For *in vivo* applications, grippers triggered at 37ºC would close on thermal equilibration with body temperature. In these cases, if needed, low-temperature storage and delivery could extend the time for autonomous thermal triggering. Alternatively, for on-demand actuation, the grippers could be engineered with wax materials that soften at a slightly higher temperature (e.g. 39-40ºC). Since the grippers contain a layer of dense and magnetic iron, they offer the possibility for remote coupling to electromagnetic and acoustic fields and induction heating or high-intensity focused ultrasound could be exploited to remotely and specifically heat heat the grippers and minimize collateral thermal damage.

Our fabrication process is highly reproducible, scalable and compatible with microchip industry for cost-effective fabrication. We note that approximately 200,000 grippers fit on a 3-inch wafer with feasible scale up to millions on larger wafers in semiconductor foundries. The wafer scale fabrication also offers the possibility for future integration of optical or electronic modules,[22, 23] so that biosensing, decision making, and surgical intervention can potentially be performed simultaneously *in situ*. It is also conceivable that antibodies could be patterned to target specific cells for autonomous sampling. Furthermore, with enhanced microfabrication resolution, additional hinges per finger could be incorporated for more complex motions including opening up to release captured objects. Finally, the use of bioresorbable films such as SiO, SiO_2 and Fe[37, 38] offer the possibility to create devices that could degrade within the human body which is important from a safety perspective.

ASSOCIATED CONTENT

Supporting Information

The Supporting Information is available free of charge on the website at DOI, which includes detailed experimental methods, additional data and mechanical analysis (PDF).

Supporting Movie 1: Video showing a gripper picking and moving a single cell.

Supporting Movie 2: Video of a gripper excising a few cells from a cluster.

AUTHOR INFORMATION

Corresponding Author

*E-mail: dgracias@jhu.edu.

Notes

Under an option to license agreement between Kley Dom Biomimetics, LLC and the Johns Hopkins University, Prof. D. H. Gracias and the Johns Hopkins University are entitled to royalty distributions related to technology described in the study discussed in this publication. This arrangement has been reviewed and approved by the Johns Hopkins University in accordance with its conflict of interest policies.

ACKNOWLEDGMENTS

We would like to thank Dr. Evin Gultepe and YooSun Shim for helpful suggestions related to the micropatterning of paraffin wax and to Dr. Arijit Ghosh for discussions on magnetic gradient field estimation. We acknowledge support from the National Science Foundation NSF CMMI 1635443. We also acknowledge support from the National Institute of Biomedical Imaging and Bioengineering (NIBIB) of the National Institutes of Health (NIH) under award number R01EB017742. The content is solely the responsibility of the authors and does not necessarily represent the official views of the National Institutes of Health.

References

1. Ceylan, H.; Giltinan, J.; Kozielski, K.; Sitti, M. Mobile microrobots for bioengineering applications. *Lab. Chip* **2017,** *17*, 1705-1724.
2. Avila, B.E.-F.D.; Gao, W.; Karshalev, E.; Zhang, L.; Wang, J. Cell-Like Micromotors. *Acc. Chem. Res.* **2018,** *51*, 1901-1910.
3. Soto, F.; Chrostowski, R. Frontiers of Medical Micro/Nanorobotics: in vivo Applications and Commercialization Perspectives Toward Clinical Uses. *Front. Bioeng. Biotechnol.* **2018,** *6*, 170.
4. Nelson, B. J.; Kaliakatsos, I. K.; Abbott, J. J. Microrobots for minimally invasive medicine. *Annu. Rev. Biomed. Eng.* **2010,** *12*, 55-85.
5. Lawson, D. A.; Bhakta, N. R.; Kessenbrock, K.; Prummel, K. D.; Yu, Y.; Takai, K.; Zhou, A.; Eyob, H.; Balakrishnan, S.; Wang, C. Y.; Yaswen, P.; Goga, A.; Werb, Z. Single-cell analysis reveals a stem-cell program in human metastatic breast cancer cells. *Nature* **2015,** *526*, 131-135.
6. Park, J.; Shrestha, R.; Qiu, C.; Kondo, A.; Huang, S.; Werth, M.; Li, M.; Barasch, J.; Susztak, K. Single-cell transcriptomics of the mouse kidney reveals potential cellular targets of kidney disease. *Science* **2018,** *360*, 758-763.
7. Ichikawa, A.; Sakuma, S.; Sugita, M.; Shoda, T.; Tamakoshi, T.; Akagi, S.; Arai, F. On-chip enucleation of an oocyte by untethered microrobots. *J. Micromech. Microeng.* **2014,** *24*, 095004.
8. Medina-Sánchez, M.; Schwarz, L.; Meyer, A. K.; Hebenstreit, F.; Schmidt, O. G. Cellular cargo delivery: Toward assisted fertilization by sperm-carrying micromotors. *Nano Lett.* **2016,** *16*, 555-561.
9. Matuła, K.; Rivello, F.; Huck, W. T. Single-Cell Analysis Using Droplet Microfluidics. *Adv. Biosyst.* **2020,** *4*, 1900188.
10. Chen, P.; Güven, S.; Usta, O. B.; Yarmush, M. L.; Demirci, U. Biotunable acoustic node assembly of organoids. *Adv. Healthcare Mater.* **2015,** *4*, 1937-1943.
11. Ávila, B. E.-F.D.; Angsantikul, P.; Li, J.; Lopez-Ramirez, M. A.; Ramírez-Herrera, D. E.; Thamphiwatana, S.; Chen, C.; Delezuk, J.; Samakapiruk, R.; Ramez, V. Micromotor-enabled active drug delivery for in vivo treatment of stomach infection. *Nat. Commun.* **2017,** *8*, 1-9.
12. Kagan, D.; Benchimol, M. J.; Claussen, J. C.; Chuluun-Erdene, E.; Esener, S.; Wang, J. Acoustic droplet vaporization and propulsion of perfluorocarbon-loaded microbullets for targeted tissue penetration and deformation. *Angew. Chem., Int. Ed. Engl.* **2012,** *51*, 7519-7522.
13. Solovev, A. A.; Xi, W.; Gracias, D. H.; Harazim, S. M.; Deneke, C.; Sanchez, S.; Schmidt, O. G. Self-propelled nanotools. *ACS Nano* **2012,** *6*, 1751-1756.
14. Wang, W.; Li, S.; Mair, L.; Ahmed, S.; Huang, T. J.; Mallouk, T. E. Acoustic propulsion of nanorod motors inside living cells. *Angew. Chem., Int. Ed. Engl.* **2014,** *53*, 3201-3204.
15. Xu, X.; Kim, K.; Li, H.; Fan, D. L. Ordered arrays of Raman nanosensors for ultrasensitive and location predictable biochemical detection. *Adv. Mater.* **2012,** *24*, 5457-5463.
16. Fan, D.; Yin, Z.; Cheong, R.; Zhu, F. Q.; Cammarata, R. C.; Chien, C.; Levchenko, A. Subcellular-resolution delivery of a cytokine through precisely manipulated nanowires. *Nat. Nanotechnol.* **2010,** *5*, 545.
17. Chatzipirpiridis, G.; Ergeneman, O.; Pokki, J.; Ullrich, F.; Fusco, S.; Ortega, J. A.; Sivaraman, K. M.; Nelson, B. J.; Pané, S. Electroforming of implantable tubular magnetic microrobots for wireless ophthalmologic applications. *Adv. Healthcare Mater.* **2015,** *4*, 209-214.
18. Pal, M.; Somalwar, N.; Singh, A.; Bhat, R.; Eswarappa, S. M.; Saini, D. K.; Ghosh, A. Maneuverability of magnetic nanomotors inside living cells. *Adv. Mater.* **2018,** *30*, 1800429.
19. Sakar, M. S.; Steager, E. B.; Kim, D. H.; Kim, M. J.; Pappas, G. J.; Kumar, V. Single cell manipulation using ferromagnetic composite microtransporters. *Appl. Phys. Lett.* **2010,** *96*, 043705.
20. Xi, W.; Solovev, A. A.; Ananth, A. N.; Gracias, D. H.; Sanchez, S.; Schmidt, O. G. Rolled-up magnetic microdrillers: towards remotely controlled minimally invasive surgery. *Nanoscale* **2013,** *5*, 1294-1297.
21. Malachowski, K.; Jamal, M.; Jin, Q.; Polat, B.; Morris, C. J.; Gracias, D. H. Self-folding single cell grippers. *Nano Lett.* **2014,** *14*, 4164-4170.

22. Jin, Q.; Li, M.; Polat, B.; Paidi, S. K.; Dai, A.; Zhang, A.; Pagaduan, J. V.; Barman, I.; Gracias, D. H. Mechanical Trap Surface-Enhanced Raman Spectroscopy for Three-Dimensional Surface Molecular Imaging of Single Live Cells. *Angew. Chem., Int. Ed. Engl.* **2017,** *56*, 3822-3826.
23. Cools, J.; Jin, Q.; Yoon, E.; Alba Burbano, D.; Luo, Z.; Cuypers, D.; Callewaert, G.; Braeken, D.; Gracias, D. H. A Micropatterned Multielectrode Shell for 3D Spatiotemporal Recording from Live Cells. *Adv. Sci.* **2018,** *5*, 1700731.
24. Gultepe, E.; Randhawa, J. S.; Kadam, S.; Yamanaka, S.; Selaru, F. M.; Shin, E. J.; Kalloo, A. N.; Gracias, D. H. Biopsy with thermally-responsive untethered microtools. *Adv. Mater.* **2013,** *25*, 514-519.
25. Noti, A.; Grob, K.; Biedermann, M.; Deiss, U.; Brüschweiler, B. J. Exposure of babies to C15–C45 mineral paraffins from human milk and breast salves. *Regul. Toxicol. Pharmacol.* **2003,** *38*, 317-325.
26. Hyun, D. C.; Levinson, N. S.; Jeong, U.; Xia, Y. Emerging applications of phase-change materials (PCMs): teaching an old dog new tricks. *Angew. Chem., Int. Ed. Engl.* **2014,** *53*, 3780-3795.
27. Liu, R. H.; Bonanno, J.; Yang, J.; Lenigk, R.; Grodzinski, P. Single-use, thermally actuated paraffin valves for microfluidic applications. *Sens. Actuators, B* **2004,** *98*, 328-336.
28. Carlen, E.; Mastrangelo, C. In *Paraffin actuated surface micromachined valves*, Proceedings IEEE Thirteenth Annual International Conference on Micro Electro Mechanical Systems, Miyazaki, Japan, Jan 23-27, 2000; IEEE: Piscataway, NJ, 2000.
29. Shim, Y. Diagnostics and Therapeutics Using Untethered Microgrippers. M.S.E. Thesis, Johns Hopkins University, Baltimore, MD, 2013.
30. Craig, R.; Eick, J.; Peyton, F. Strength properties of waxes at various temperatures and their practical application. *J. Dent. Res.* **1967,** *46*, 300-305.
31. Nakano, T.; Yoshida, K.; Ikeda, S.; Oura, H.; Fukuda, T.; Matsuda, T.; Negoro, M.; Arai, F. In *Fabrication of Transparent Arteriole Membrane Models*, Proceedings of 2008 International Symposium on Micro-NanoMechatronics and Human Science, Nagoya, Japan, Nov 6-9, 2008 IEEE: Piskataway, NJ, 2008.
32. Nikishkov, G. P. Curvature estimation for multilayer hinged structures with initial strains. *J. Appl. Phys.* **2003,** *94*, 5333-5336.
33. Ongaro, F.; Scheggi, S.; Ghosh, A.; Denasi, A.; Gracias, D. H.; Misra, S. Design, characterization and control of thermally-responsive and magnetically-actuated micro-grippers at the air-water interface. *PloS One* **2017,** *12*.
34. Intengan, H. D.; Schiffrin, E. L. Structure and mechanical properties of resistance arteries in hypertension: role of adhesion molecules and extracellular matrix determinants. *Hypertension* **2000,** *36*, 312-318.
35. Jones, A.; Knudsen, J. G. Drag coefficients at low Reynolds numbers for flow past immersed bodies. *AIChE J.* **1961,** *7*, 20-25.
36. Utsushikawa, Y.; Niizuma, K. The saturation magnetization of Fe-N films prepared by nitriding treatment in N2 plasma. *J. Alloys Compd.* **1995,** *222*, 188-192.
37. Hwang, S.-W.; Tao, H.; Kim, D.-H.; Cheng, H.; Song, J.-K.; Rill, E.; Brenckle, M. A.; Panilaitis, B.; Won, S. M.; Kim, Y.-S. A physically transient form of silicon electronics. *Science* **2012,** *337*, 1640-1644.
38. Kang, S. K.; Hwang, S. W.; Cheng, H.; Yu, S.; Kim, B. H.; Kim, J. H.; Huang, Y.; Rogers, J. A. Dissolution behaviors and applications of silicon oxides and nitrides in transient electronics. *Adv. Funct. Mater.* **2014,** *24*, 4427-4434.

Supporting Information

Untethered Single Cell Grippers for Active Biopsy

Qianru Jin,[1, ∀] Yuqian Yang,[1] Julian A. Jackson,[1] ChangKyu Yoon,[2, #] David H. Gracias[1, 2, *]

[1]Department of Chemical and Biomolecular Engineering, Johns Hopkins University, Baltimore, Maryland 21218, United States

[2]Department of Materials Science and Engineering, Johns Hopkins University, Baltimore, Maryland 21218, United States

[∀]Present address: Disease Biophysics Group, John A. Paulson School of Engineering and Applied Sciences, Harvard University, Cambridge, MA 02138, USA

[#]Present address: Department of Mechanical Systems Engineering, Sookmyung Women's University, Seoul, 04310, Republic of Korea

Supplementary methods and models

1. Fabrication process of the single cell grippers

We fabricated the grippers based on previously reported methods,[21,22] with the introduction of new functional layers. Briefly, we first deposited a sacrificial layer of copper (Cu) on a bare silicon (Si) wafer; the sacrificial layer facilitates the release of the grippers from the wafer after fabrication. Second, we photopatterned and deposited a bilayer of silicon monoxide and silicon dioxide by e-beam evaporation. The release of energy from this differentially stressed bilayer drives self-folding of the grippers. In this study, we used a bilayer of 10 nm silicon monoxide (Kurt J Lesker, EVMSIO-1065B) and 20 nm silicon dioxide (Kurt J Lesker, EVMSIO21-5D) to achieve the desired fold angle. Third, we photopatterned thicker rigid segments composed of 100 nm silicon dioxide and 100 nm iron (Kurt J Lesker, EVMFE35QXQD) by e-beam evaporation. Next, we patterned the paraffin (details in the following section). After fabrication, we released the grippers from the substrate by dissolving the Cu sacrificial layer in a commercial Cu etchant ammonium persulfate (APS-100, Transene). Prior to their release from the wafer, we rinsed the grippers for three times with PBS to remove residual APS.

2. Paraffin patterning

The first two fabrication steps for the stress layer and the rigid segments establish the basic components of the grippers. Next, we patterned paraffin wax as a thermally responsive layer to trigger the folding of grippers on heating. First, we patterned a photoresist mold to define the shape and thickness of the paraffin. We spin coated S1813 photoresist on the silicon wafer at 3000 rpm. After soft bake at 115°C for 1 min, we aligned a photomask with the wafer using registry marks, so as to expose the resist only in the regions of the grippers to UV light with an energy of 150 mJ/cm^2. We then developed the exposed photoresist in AZ 319 MIF developer to leave behind photoresist only in the regions without the grippers.

We first melted the paraffin wax (Sigma, 411663) at 120°C. We then placed the patterned wafer on the chuck inside the spin coater, and held a heat gun at a distance and towards the wafer to heat it to approximately 140°C. We quickly dispensed 1 mL of liquid wax onto the patterned wafer and started the spin coating cycle while continuing to direct the heat source during spin coating. We spincoated the molten wax at 5000 rpm for 1 min and then cooled the wafer in air overnight. After wax coating and cooling, we washed the wafer in acetone, and then rinsed the wafer in isopropyl alcohol (IPA) and deionized water to remove the underlying photoresist. After this process, the remaining paraffin wax covers only the region of the grippers and the grippers are ready to be released and used. For butter triggered grippers, we patterned food grade butter on the grippers using a similar method but at a lower temperature.

3. Microfluidic chamber fabrication, and gripper actuation

We fabricated microfluidic chambers to investigate guidance of single cell grippers through narrow, bifurcated, and winding channels. We designed the channel patterns in AutoCAD and transferred them to a photomask. Then, we pretreated a clean Si wafer with hexamethyldisilazane (HMDS) and spin coated SU8 2050 at 1700 rpm to create a 100 μm thick pattern. After soft baking at 65°C for 5 min and 95°C for 15 min, we exposed the wafer to 240 mJ/cm^2 UV light through the photomask to transfer the pattern from the photomask to the SU8. We post exposure baked the wafer at 65°C for 5 min and 95°C for 10 min and then developed the patterns in SU8 developer for another 10 min. We rinsed the wafer with IPA and DI water, and then hard baked the SU8 resist at 200°C for 30 min.

We thoroughly mixed PDMS elastomer and the curing agent (Dow Corning) at a ratio of 10:1 and degassed the solution in a desiccator for at least 2 hours before pouring the mixture onto the pattern. We cured the PDMS at 75°C overnight. After curing, we used a blade to cut and peel the PDMS patterns off. We punched holes in the patterned PDMS using a 1.5 mm portable biopsy punch at designated positions

and then treated the PDMS interface with an oxygen plasma. We then bonded a glass slide to the PDMS to seal the channels. The microfluidic chamber was then ready to use.

To trigger gripper actuation, we applied heat by one of three methods; either by warming up the solution on a hot plate during imaging with an upright microscope, or by directing heat with a heat gun during imaging on an inverted microscope or using a temperature-controlled chamber in a confocal microscope. When we used a hot plate, we added the cells and released grippers in PBS in a small dish, and placed the dish on a hot plate. We inserted a digital probe into the dish to monitor the temperature change during the gripper folding process. First, at room temperature, we steered the gripper towards the targeted cells using a magnetic field. When the gripper reached the desired location, we turned on the hot plate to a pre-calibrated setting to increase the temperature. For fast actuation and high-resolution imaging under inverted microscope, we used a heat gun to apply heat remotely and used the digital temperature probe to monitor the temperature. For live cell imaging in the single cell grippers we heated the solution using a temperature-controlled chamber. In this study, we estimate the gripper trigger temperature to be 37±2ºC and attribute the standard deviation to variations in the paraffin wax thickness. For *in vivo* applications which require remote heat delivery, we envision methods such as induction heating or high-intensity focused ultrasound to selectively heat the iron-containing grippers to deliver the heat specifically and minimize collateral damage.

4. Cell culture and cell cluster preparation

We maintained WI-38 human fetal lung fibroblasts in Minimal Essential Medium (Corning Cellgro, 10-010-CV) supplemented with 10% fetal bovine serum (FBS; Thermo Fisher, 16140071), 1% penicillin-streptomycin (Thermo Fisher, 15140122), 1% sodium pyruvate (MilliporeSigma, S8636) and 1% non-essential amino acids (MilliporeSigma, M7145). We maintained the breast cancer cell line MDA-MB-231 in DMEM with 10% FBS and 1% penicillin-streptomycin.

We cultured fibroblasts until a desired confluence was reached (80%). After removing the culture media, we added 1mL trypsin to retrieve the adherent cells. We then centrifuged the cell suspension at 1000 rpm for 3 min. Instead of resuspending the cells, we extracted 10 μL of the mixture from the bottom of the tube and used it as the cell cluster in our cell excision experiments.

5. Cell staining, fluorescence imaging and live/dead assay

We permeabilized the cells using 0.1% Triton-X in a 4% paraformaldehyde (PFA) solution for 2 min and fixed the cells using a 4% PFA solution for 20 min. We stained the cells for β-tubulin using antibody (Abcam, ab6046, 1:100 dilution) and Alexa Fluor 488 (Jackson ImmunoResearch, 111-545-003, 1:100 dilution), and nuclei using 0.1% DAPI (Thermo Fisher, 62248).

For the live/dead assay during the gripper closing process, we first rinsed and trypsinized the adherent cells, and collected and incubated them with PBS containing 1 μM calcein AM and 2 μM ethidium homodimer-1 for 30 minutes. Next, we added about 200 μL cell solution to a small dish for imaging and a droplet containing the released grippers in PBS to the solution. We placed the dish in a temperature-controlled chamber for simultaneous confocal fluorescence microscopy and gripper actuation. We triggered the gripper closing by increasing the temperature in the chamber from room temperature to 37ºC using the controlled heating blocks in the chamber. We monitored the fluorescence signals from the cells continuously throughout and after the gripper closing process.

6. Ex-vivo tissue preparation

We purchased tissue microscope slides from Carolina Biological Supply Company (Item # 316102). We disassembled the slides in order to remove the coverslip and to allow accessibility of the grippers to the tissue. Once we removed the coverslip, we added a drop of gripper-containing solution onto the tissue.

7. Dynamic Mechanical Analysis (DMA)

We molded and used ~1 cm^3 paraffin cubes for DMA measurements. To obtain elastic moduli values for the wax at different temperatures, we stabilized the chamber temperature for more than 30 min to reach a steady temperature. We subjected the samples to an unconfined compression, controlled force deformation test (Q800 DMA, TA instruments). We increased the applied force at a rate of 2 N/min until a maximum static force of 2 N, after which we reduced the load at a rate of 4 N/min to 0 N.

8. Fold angle analysis by analytical solution and finite element analysis

We modeled the fold angle of the grippers using an analytical solution adopted from the literature,[32] and finite element analysis. We considered the hinge to be composed of three layers: silicon monoxide, silicon dioxide and paraffin. We estimated the differential strain in the bilayer to be 0.0043 based on a previous study.[21] The material properties used are listed below in the format as: material (Young's modulus, Poisson's ratio, thickness). Silicon monoxide (77 GPa, 0.2, 10 nm), silicon dioxide (75 GPa, 0.17, 20 nm), cold paraffin (6.44 MPa, 0.2, variable) and warm paraffin (0.37 MPa, 0.2, variable).

For finite element analysis (FEA), we used a shell model to construct the gripper, due to the large ratio between the lateral dimensions and the thickness. We adopted the model from a prior publication.[21] We based the gripper dimensions on the AutoCAD design. We defined the thickness of the flexible hinge as described in the previous paragraph. We used a static model and considered non-linear deformation to capture the large deformation. We used a mesh size of 2 μm and the element type of S4R in the model. We performed a convergence study to verify that a further increase of mesh numbers did not change the results. We set the boundary conditions as below. 1: We fixed the x-axis and y-axis at the center of the gripper to be dx = dy = dz = 0; 2: We considered the x-axis and y-axis throughout the gripper to be y-symmetrical and x-symmetrical. We assigned a thermal expansion coefficient to the silicon monoxide layer and applied a temperature field only at the hinge, to simulate the differential stress between the bilayer. We used a strain difference of 0.0043 based on the previous measurement.[21]

9. Estimation of the magnetic field gradient to move the single cell grippers

We used an analytical model to estimate the magnetic field gradient that is needed to move the single cell grippers in a fluid environment. We based the analysis on a model from a previous study.[33]

If we assume that the micro-object is suspended in liquid without friction with solid surface, we can write the translational equations of motion in the planar workspace as:

$$F_{em} + F_d + F_i = 0 \quad (1)$$

where F_{em} is the electromagnetic force, F_d is the drag force, and F_i is the inertial force. In the case of single cell grippers, where speed $v = 100\ \mu m/s$, feature length $L = 70\ \mu m$, water density $\rho = 1 \times 10^3\ kg/m^3$, and water viscosity $\mu = 8.90 \times 10^{-4}\ Pa \cdot s$ at 25ºC, the Reynolds number,

$$Re = \rho \frac{L\,v}{\mu} = 7.86 \times 10^{-3} < 0.01$$

When the Reynolds number $Re < 0.01$, we can neglect the inertial force relative to the other forces. With this assumption that F_i is negligible, equation (1) becomes,

$$F_{em} + F_d = 0 \quad (2)$$

Since the grippers move at sub-centimeter speeds in a flow-less environment, we can write an equation for F_d as,

$$F_d = \frac{1}{2}\rho C_D A v^2 = 2 \times 10^{-13}\ N$$

where the fluid density $\rho = 1 \times 10^3\ kg/m^3$, cross sectional area normal to the direction of motion $A = 82\ \mu m^2$ and the speed of the gripper $v = 100\ \mu m/s$. We can estimate the drag coefficient C_D to be $C_D = 500$ based on prior studies of the drag coefficient of a plate in a parallel flow at Re = 0.01.[35]

Considering the unidirectional motion of gripper, we can write an equation for the electromagnetic force in the one-dimensional magnetic gradient field as,

$$F_{em} = \nabla\,(m \cdot B) = m \cdot \nabla \mathrm{B}$$

We can also estimate the magnetic dipole moment m as,

$$m = M_s \cdot V = 1.2 \times 10^{-10} A \cdot m^2$$

where the iron material volume $V = 7 \times 10^{-17}\ m^3$, saturation magnetization M_s for the approximately 100 nm thick iron thin film is $M_s = 1.7\ \times 10^6\ A/m$.[36]

Hence, we can estimate the required magnetic field gradient ∇B to move the single cell gripper to be,

$$\nabla \mathrm{B} = -\frac{F_d}{m} = -1.6 \times 10^{-3}\ T/m$$

Supplementary figures

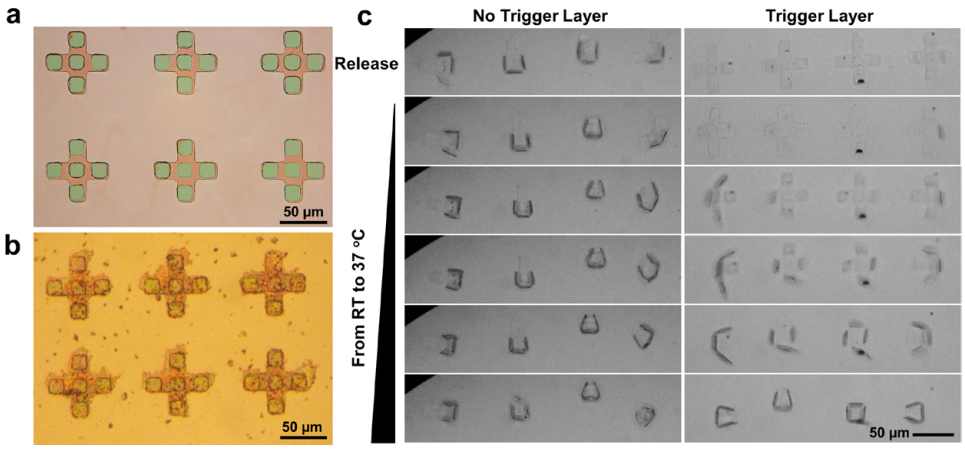

Figure S1. Butter as the trigger layer for thermal actuation of single cell grippers. **(a)** Optical image of a control sample containing an array of grippers with square arms fabricated without a butter coating. The arms contain 100 nm of silicon dioxide and 100 nm of iron. **(b)** Optical image of an array of grippers coated with a thin layer of butter on top of the grippers. **(c)** Optical images showing the folding process of grippers without butter (left), and with butter (right). After release, grippers without the trigger layer closed immediately, while grippers with trigger layer stayed open. As the temperature was increased from room temperature to 37°C, the grippers with the butter trigger layer started to close, when the butter softened.

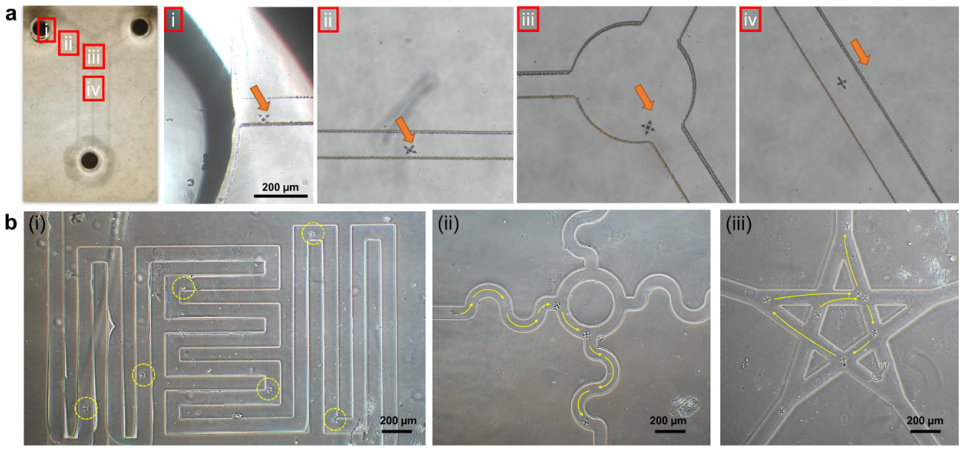

Figure S2. Grippers moving in narrow, bifurcated, and winding microfluidic channels guided by a magnetic field. (a) Optical images of a gripper navigated through a microfluidic channel with bifurcations. An overview of the microfluidic channel followed by details of the gripper: (i) leaving the initial chamber, (ii) moving through the channel, (iii) reaching the mixing chamber, (iv) exiting the mixing chamber. **(b)** Optical images of grippers being navigated through microfluidic channels of different configurations. The images show the motion path of a gripper at multiple time points, in, (i) a zig-zag channel, (ii) a twisted channel, and (iii) a star-shaped channel with many exits.

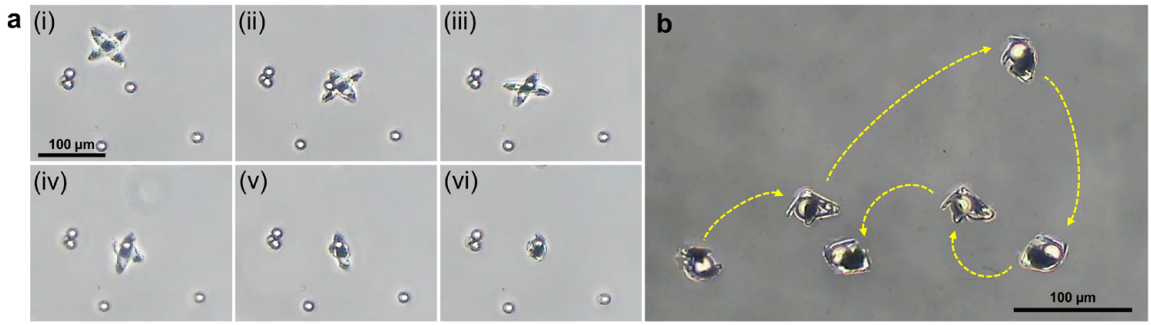

Figure S3. Grippers capturing microbeads by magnetic guidance and thermal actuation. (a) (i-iii) Optical image sequence showing a gripper approaching a polystyrene microbead (15 µm diameter) from a distance guided by the magnetic field; (iv-vi) The gripper started closing and captured the bead upon temperature increase. **(b)** Optical image sequence showing a gripper carrying the microbead guided by the magnetic field and navigating through an arbitrary trace.

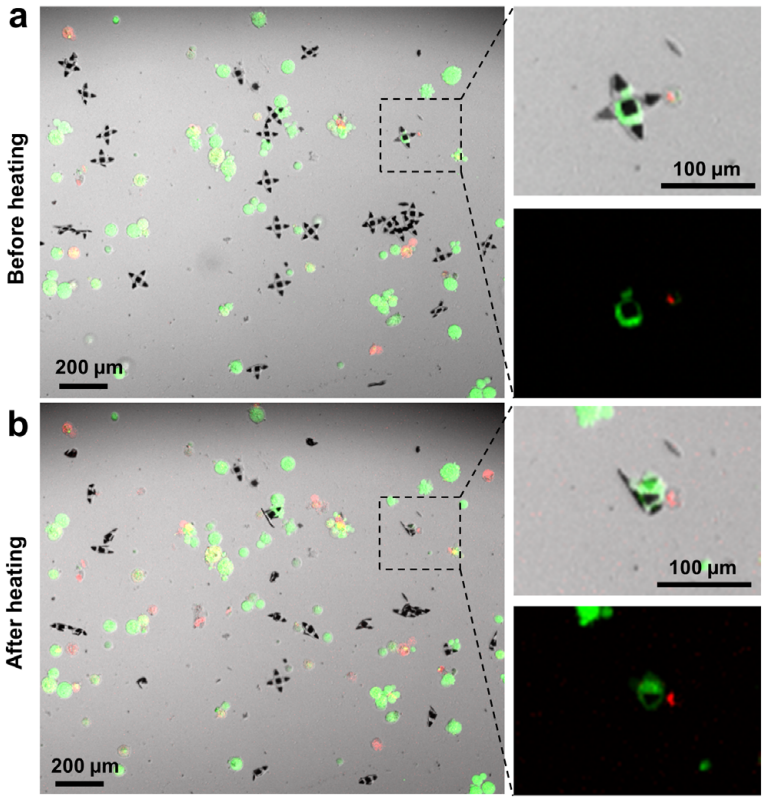

Figure S4. Biocompatibility of the self-folding process. (a) Optical fluorescence microscopy images showing grippers and cells that were stained by calcein AM and ethidium homodimer for a live/dead assay. The green fluorescence indicates live cells and red color indicates dead cells. **(b)** Optical fluorescence microscopy images showing that a majority of cells remained alive after temperature increase from room temperature to 37°C. A few cells with red fluorescence were from the sediment of suspended dead cells. The right zoom-in images show a gripper capturing a single cell. The time interval between the acquisition of the two images was approximately 30 minutes, with calcein AM and ethidium homodimer present in the solution throughout the process.

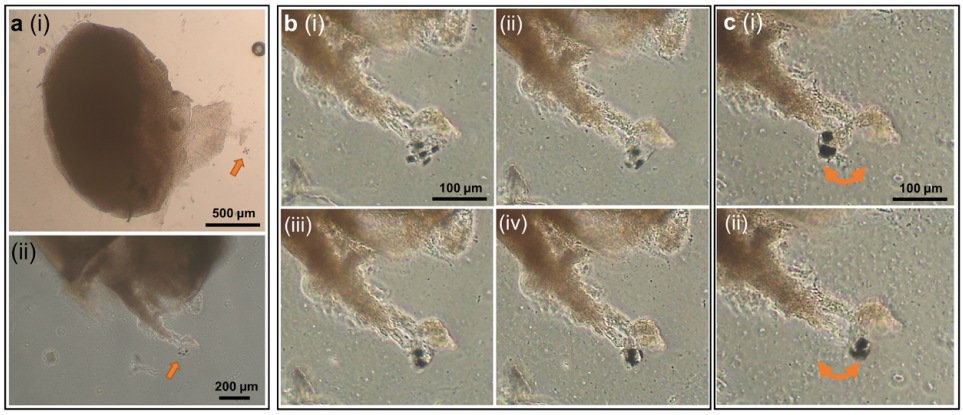

Figure S5. Grippers pulling liver tissue by magnetic locomotion and thermal actuation. (a) Optical image of a gripper approaching a piece of chicken liver tissue from a remote distance and reaching its periphery, guided by a magnetic field. **(b)** Optical image sequence showing the gripper folding and holding onto a piece of tissue upon temperature increase. **(c)** Optical image sequence showing that the gripper firmly grasped the tissue and generated large dislocation with strong dragging and twisting motion, steered by the magnetic field.

References

21. Malachowski, K.; Jamal, M.; Jin, Q.; Polat, B.; Morris, C. J.; Gracias, D. H. Self-folding single cell grippers. *Nano Lett.* **2014**, *14*, 4164-4170.

22. Jin, Q.; Li, M.; Polat, B.; Paidi, S. K.; Dai, A.; Zhang, A.; Pagaduan, J. V.; Barman, I.; Gracias, D. H. Mechanical Trap Surface-Enhanced Raman Spectroscopy for Three-Dimensional Surface Molecular Imaging of Single Live Cells. *Angew. Chem., Int. Ed.* **2017**, *56*, 3822-3826.

32. Nikishkov, G. P. Curvature estimation for multilayer hinged structures with initial strains. *J. Appl. Phys.* **2003**, *94*, 5333-5336.

33. Ongaro, F.; Scheggi, S.; Ghosh, A.; Denasi, A.; Gracias, D. H.; Misra, S. Design, characterization and control of thermally-responsive and magnetically-actuated micro-grippers at the air-water interface. *PLoS One* **2017**, *12*, e0187441.

35. Jones, A.; Knudsen, J. G. Drag coefficients at low Reynolds numbers for flow past immersed bodies. *AIChE J.* **1961**, *7*, 20-25.

36. Utsushikawa, Y.; Niizuma, K. The saturation magnetization of Fe-N films prepared by nitriding treatment in N2 plasma. *J. Alloys Compd.* **1995**, *222*, 188-192.